LS-282
(formerly referenced as
APS/IN/LEUTL/98-1)

Short Note on Undulator Alignments and Beam Tolerances for the APS FEL at 220 MeV

Roger J. Dejus and Isaac B. Vasserman
Experimental Facilities Division

June 1, 1998

A. Introduction

The APS FEL consists of a series of undulators that must be carefully aligned for optimum gain and high spectral output. In order to get a better understanding of acceptable tolerance levels for undulator alignments and for the electron beam, we have performed computer calculations to simulate misalignments of one undulator (undulator number 2) with respect to adjacent undulators and to check the sensitivity to unmatched beam parameters (α and β) at the entrance and to a noncentered incident beam (x_o, x_o', y_o, y_o'). We have not simulated horizontal misalignments because the undulators focus only in the vertical direction and horizontal alignments are therefore much more relaxed than vertical alignments. The exact placement and strength of the quadrupoles in the breaks need also to be addressed in follow up studies and are not presented here. Further, inherent undulator magnetic field errors have not been investigated here and will also be the subject for another study. Note, the tolerances listed in this note may be used for guidance only and will need to be updated when we have updated beam parameters.

B. Parameters

The calculations thus far were performed at one beam energy only (220 MeV) with a beam emittance of $\varepsilon_x = \varepsilon_y = 2.50 \times 10^{-8}$ m-rad and a beam energy spread (s.d.) of 0.15%. The undulator period length λ_w was 3.30 cm, and the total length of one undulator was 2.3265 m. The break length was fixed (except when longitudinal displacements were simulated) at 0.365 m with a single horizontally focusing quadrupole at the center

(with a “thin lens” focal length of 1.0/0.418 m). All undulators were ideal (no magnetic field errors) and were set to operate at a K value of 3.10 - leading to a fundamental harmonic in the visible range (5168 Å).

C. Results

The computer code used was written by R. Dejus (to be published). It solves numerically the integral equation for the electron distribution function for a high gain FEL as discussed in the Technical Bulletin ANL/APS/TB-27 by N. Vinokurov. The code has been tested and verified vs. semianalytical expressions with very good agreement. This short note summarizes our findings, and they are presented in a series of 12 tables. In Table I, we give $\ln(|J|^2)$, where J is the bunch current density for the reference run (which will show linear behavior in the exponential growth regime) and the corresponding scaling factor (slope) F of the growth. The scaling factor F is inversely related to the power gain length L_g through $F = 0.5/(K_w L_g D)$, where $K_w = 2\pi/\lambda_w$, and D is defined in the TB-27, Eq. 29 ($D = 7.0 \times 10^{-3}$ corresponding approximately to a current of 100 A). The parameter D, which depends on the current, can be written as $6.93 \times 10^{-4} \sqrt{\frac{I(A)}{E(GeV)}} \sqrt{\frac{K^2}{4+2K^2}} \times JJ(K)$ where JJ(K) is the standard combination of the zeroth and first order Bessel functions, JJ(3.1) = 0.76. The values at the exit of the second undulator (cell 2), third undulator (cell 3), and sixth undulator (cell 6) were examined as they represent two short systems (with possibly undulator number 2 displaced) and one long system (saturation effects cannot be studied, however). The values in Tables II through XI are given as the difference between the $\ln(|J|^2)$ for the actual run and the reference run. Small numbers translate directly into a percentage change of the power output, e.g., -0.10 indicates a drop of about 10%. See also figures 1 - 7, which plot the $\ln(|J|^2)$ and F vs. distance z for representative runs.

TABLE I. Reference run. Perfectly aligned undulators,

centered incident beam, and matched beam parameters at the entrance.

Reference	Cell 2	Cell 3	Cell 6
$\ln(\|J\|^2)$	2.36	3.78	7.97
F	0.24	0.24	0.24

TABLE II. Longitudinal displacements of second undulator

Displacement	Cell 2	Cell 3	Cell 6
1.0 mm [a)]	+0.01	+0.01	+0.01
10.0 mm [b)]	-0.26	-0.28	-0.26

[a)] Small increase shown is not significant.
[b)] Power loss significant; recovers quickly and remains constant (~ -0. 26).

TABLE III. Vertical displacements of second undulator

Displacement	Cell 2	Cell 3	Cell 6
50 μm [a)]	-0.01	-0.20	-1.16
50 μm [b)]	-0.20	-0.27	-0.27
100 μm [a)]	-0.05	-0.88	-4.41

[a)] No corrector magnets used in the break before and after the second undulator.
[b)] Corrector magnets used in the break before and after the second undulator.

TABLE IV. Change of α_x. Matched $\alpha_x = -0.54$.

Change in α_x	Cell 2	Cell 3	Cell 6
-0.20: +0.20	-0.08: +0.04	-0.01: -0.05	-0.06: -0.08
-0.50: +0.50	-0.24: +0.04	-0.08: -0.19	-0.25: -0.32
-1.00: +1.00	-0.53: -0.03	-0.23: -0.45	-0.67: -0.83

TABLE V. Change of α_y. Matched $\alpha_y = +0.41$.

Change in α_y	Cell 2	Cell 3	Cell 6
-0.20: +0.20	-0.06: +0.04	-0.04: +0.02	-0.07: 0.00
-0.50: +0.50	-0.22: +0.07	-0.16: 0.00	-0.35: -0.14
-1.00: +1.00	-0.74: -0.08	-0.71: -0.34	-1.52: -0.99

TABLE VI. Change of β_x. Matched $\beta_x = 2.78$ m.

Change in β_x	Cell 2	Cell 3	Cell 6
-0.20 m: +0.20 m	-0.03: +0.02	0.00: -0.01	-0.01: -0.01
-0.50 m: +0.50 m	-0.09: +0.04	-0.03: -0.03	-0.07: -0.07
-1.00 m: +1.00 m	-0.22: +0.06	-0.13: -0.10	-0.25: -0.21

TABLE VII. Change of β_y. Matched $\beta_y = 0.82$ m.

Change in β_y	Cell 2	Cell 3	Cell 6
-0.10 m: +0.10 m	0.00: -0.01	0.00: -0.02	-0.01: -0.01
-0.20 m: +0.20 m	-0.01: -0.02	-0.02: -0.04	-0.07: -0.04
-0.50 m: +0.50 m	-0.41: -0.09	-0.55: -0.17	-1.34: -0.24

TABLE VIII. Horizontal displacements of incident beam coordinate x_o

Displacement [a)]	Cell 2	Cell 3	Cell 6
200 μm	-0.05	-0.05	-0.15
500 μm	-0.29	-0.30	-0.92
1000 μm	-1.21	-1.27	-3.81

[a)] Beam focused by quadrupoles only.

TABLE IX. Vertical displacements of incident beam coordinate y_o

Displacement [a)]	Cell 2	Cell 3	Cell 6
20 μm	-0.01	-0.03	-0.06
50 μm	-0.08	-0.19	-0.35
100 μm	-0.33	-0.82	-1.50

[a)] Both undulator focusing and quadrupole defocusing.

TABLE X. Horizontal change of incident beam angle x_o'

Change	Cell 2	Cell 3	Cell 6
100 μrad	-0.06	-0.16	-0.36
200 μrad	-0.23	-0.64	-1.48
500 μrad	-1.66	-5.92	-13.51

TABLE XI. Vertical change of incident beam angle y_o'

Change	Cell 2	Cell 3	Cell 6
50 μrad	-0.10	-0.12	-0.27
100 μrad	-0.42	-0.47	-1.11
200 μrad	-2.01	-2.29	-5.92

D. Acceptable Tolerances

We summarize acceptable tolerances in Table XII based on the fact that the power output should not change more than approximately 10% for a given parameter.

TABLE XII. Acceptable tolerances

Parameter	Tolerance
Longitudinal undulator displacement	1.0 mm
Vertical undulator displacement [a)]	50 μm
Horizontal alpha function, α_x	0.20
Vertical alpha function, α_y	0.20
Horizontal beta function, β_x	0.50 m
Vertical beta function, β_y	0.20 m
Horizontal incident beam coordinate, x_o	200 μm
Vertical incident beam coordinate, y_o	50 μm
Horizontal incident beam angle, x_o'	100 μrad
Vertical incident beam angle, y_o'	50 μrad

[a)] Horizontal displacement much more relaxed: use 1.0 mm.

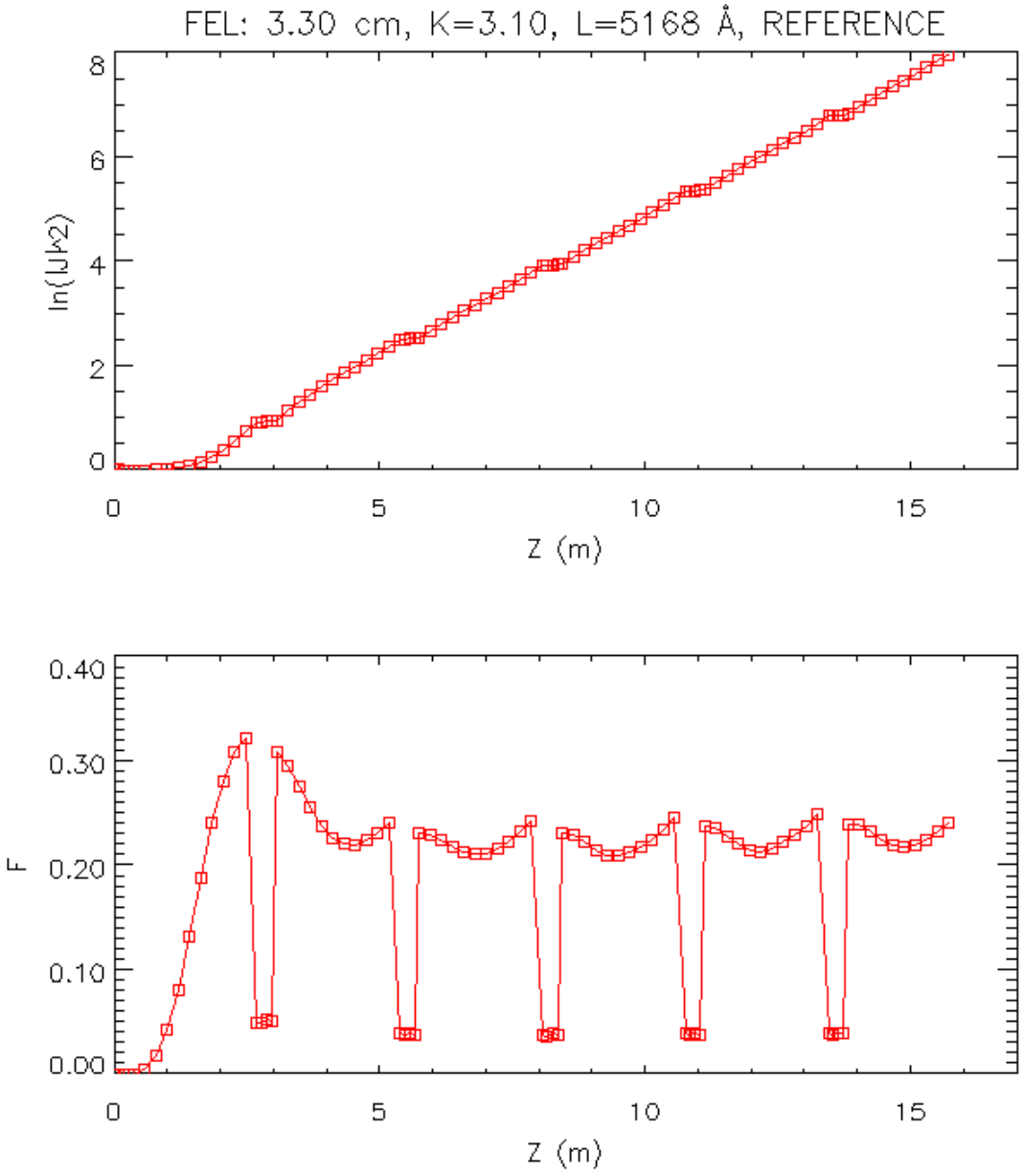

Fig. 1. Natural logarithm of the current density (top) and the scaling factor F (bottom) for the reference run. See also Table I.

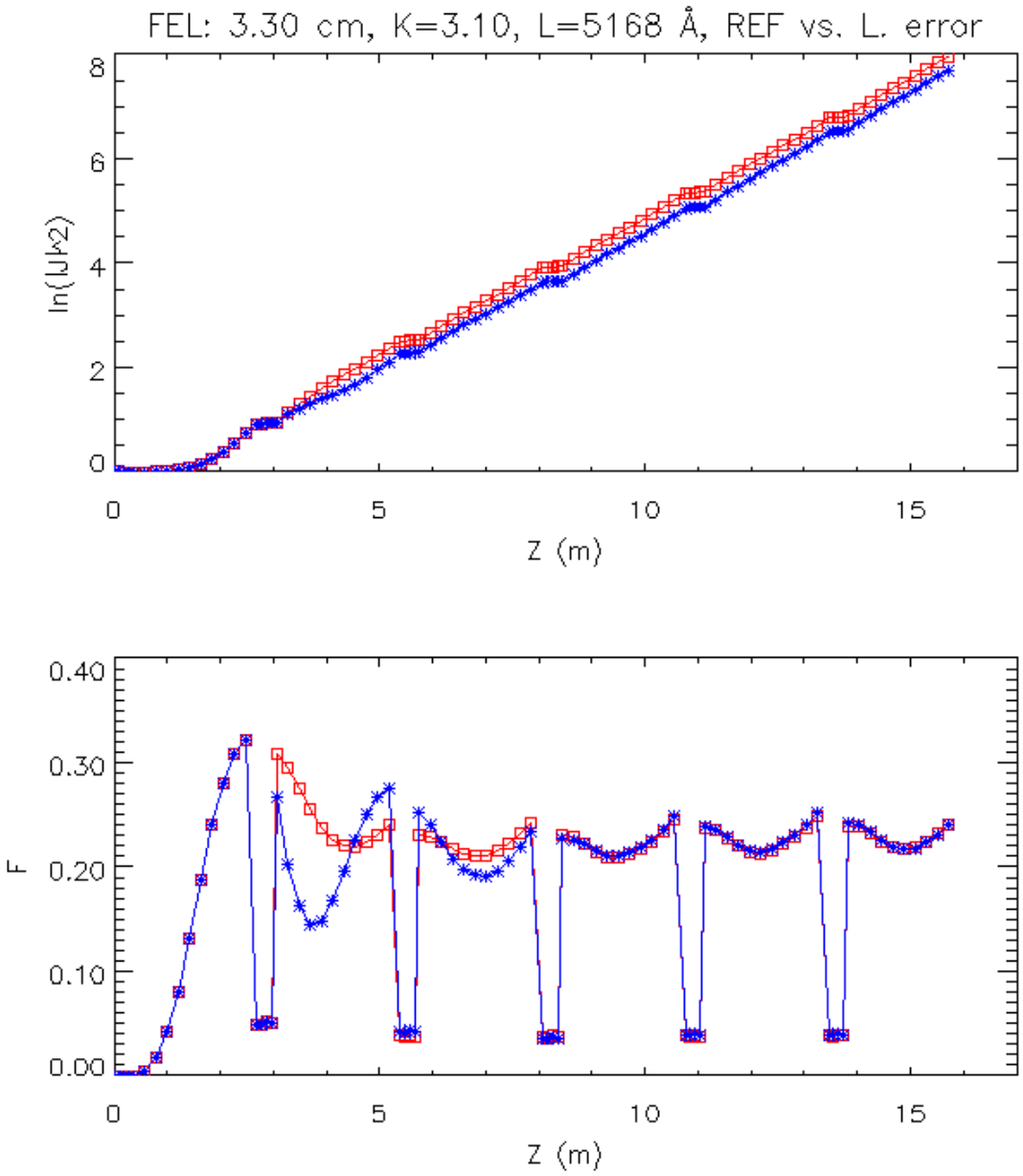

Fig. 2. Natural logarithm of the current density (top) and the scaling factor F (bottom) for the reference run (red squares) vs. the second undulator being displaced longitudinally 10.0 mm (blue stars). A small displacement of only 1.0 mm would give overlapping curves and is not shown. See also Table II.

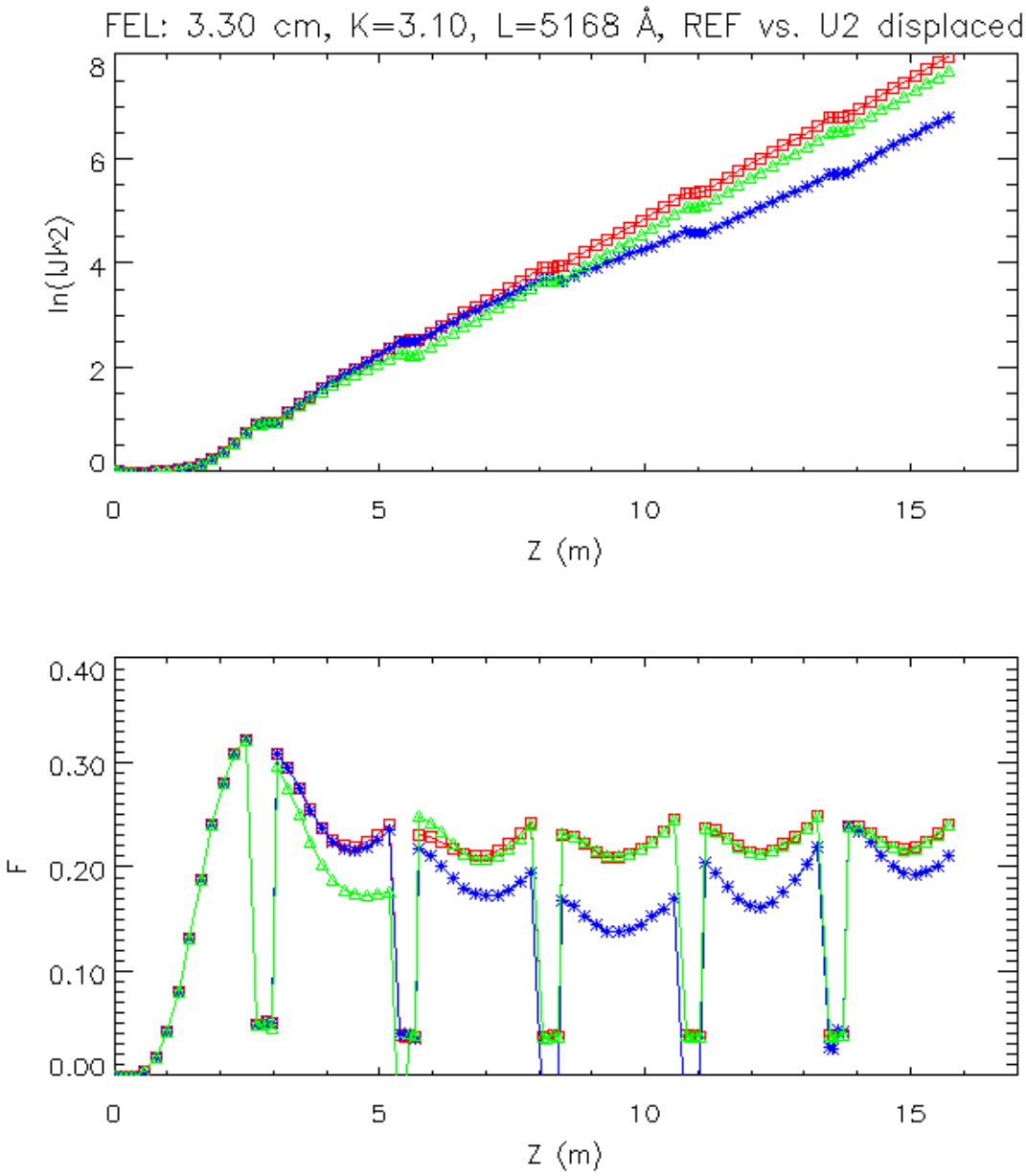

Fig. 3. Natural logarithm of the current density (top) and the scaling factor F (bottom) for the reference run (red squares) vs. the second undulator being vertically displaced 50 μm -- without corrector magnets (blue stars) and with corrector magnets (green triangles). See also Table III.

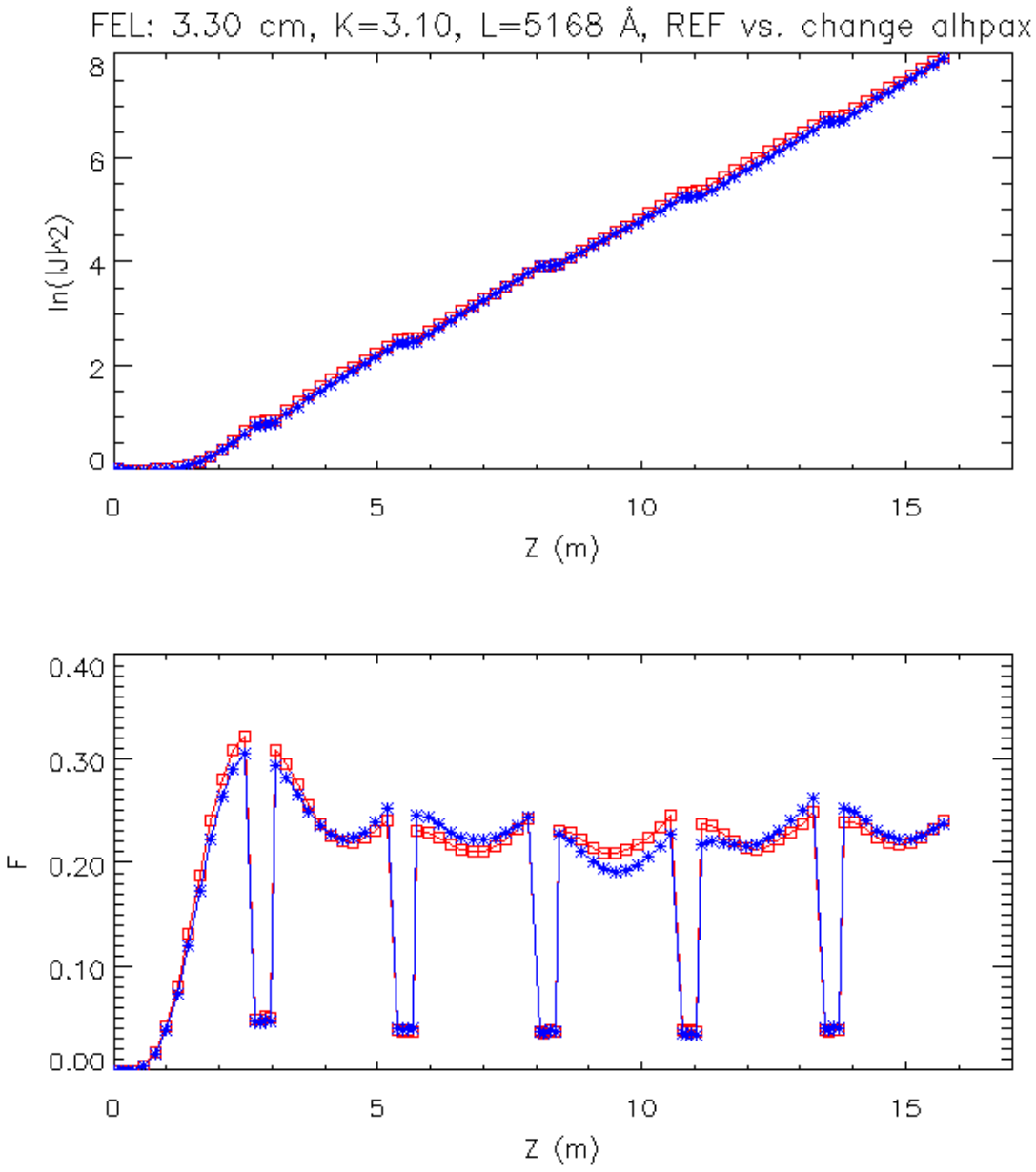

Fig. 4. Natural logarithm of the current density (top) and the scaling factor F (bottom) for the reference run (red squares) vs. a change of α_x by -0.20 (blue stars). See also Table IV.

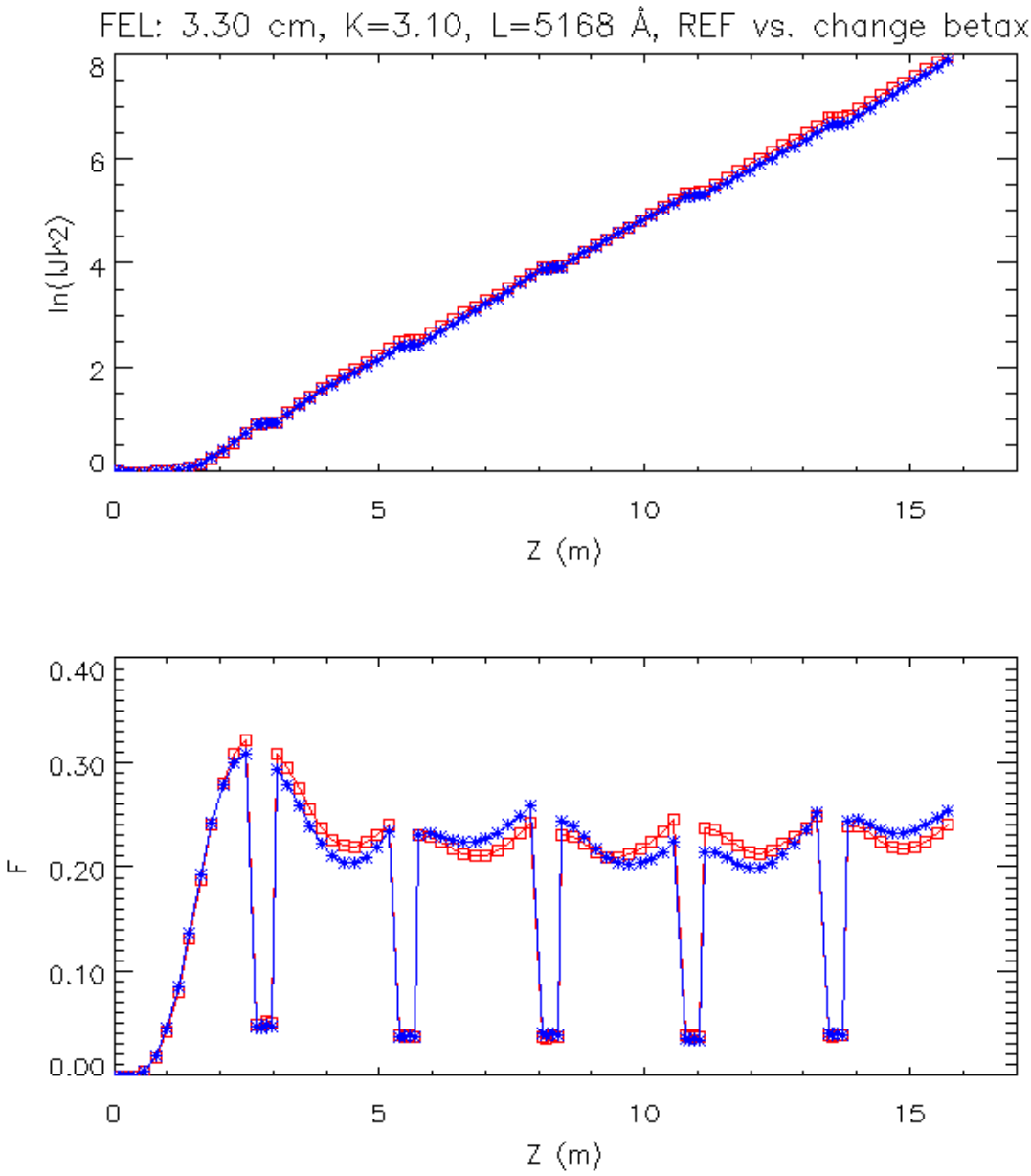

Fig. 5. Natural logarithm of the current density (top) and the scaling factor F (bottom) for the reference run (red squares) vs. a change of β_x by -0.50 m (blue stars). See also Table VI.

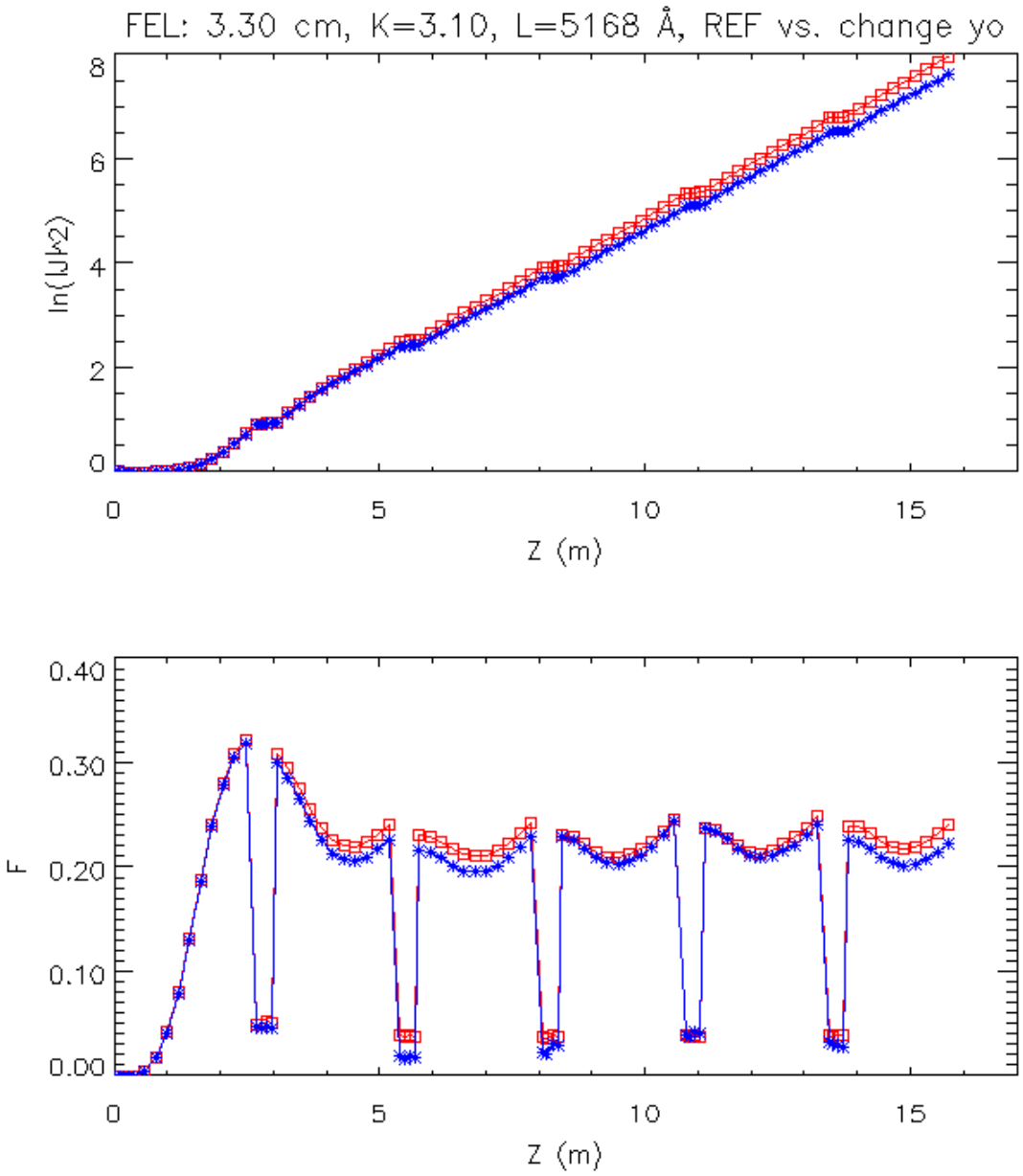

Fig. 6. Natural logarithm of the current density (top) and the scaling factor F (bottom) for the reference run (red squares) vs. a change of the vertical incident coordinate y_o by 50 μm (blue stars). See also Table IX.

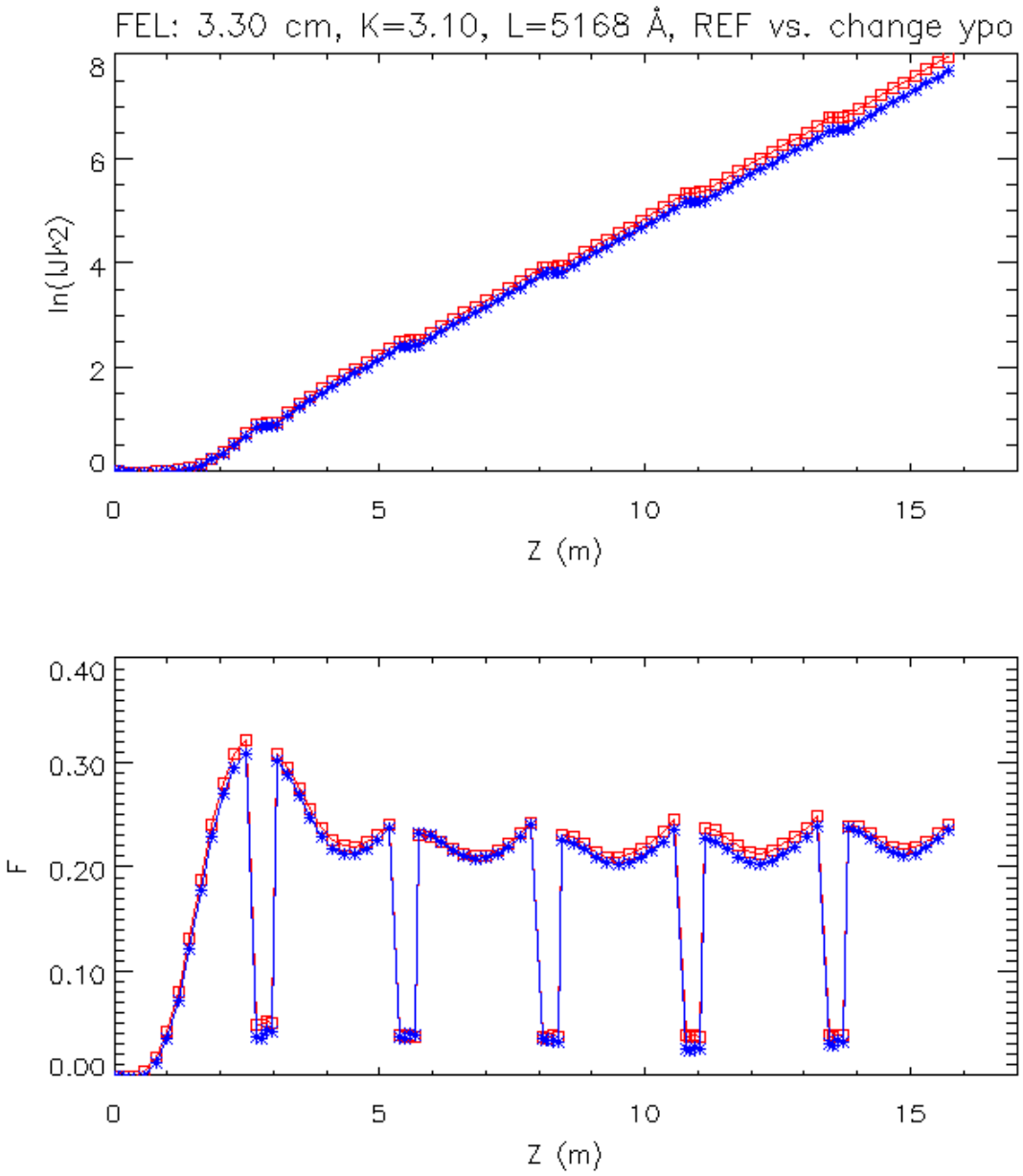

Fig. 7. Natural logarithm of the current density (top) and the scaling factor F (bottom) for the reference run (red squares) vs. a change of the vertical incident angle y_o' by 50 μrad (blue stars). See also Table XI.